https://dx.doi.org/10.1016/j.engstruct.2020.110370

Structural behaviour of stud shear connections in composite floors with various connector arrangements and profiled deck configurations

Min-hui Shen [a], Kwok-Fai Chung * [b, c], Ahmed Y. Elghazouli [d], and Jing-Zhong Tong [e]

[a] Department of Urban Construction and Safety Engineering,
Shanghai Institute of Technology, China.
[b] Department of Civil and Environmental Engineering,
the Hong Kong Polytechnic University, Hong Kong SAR, China.
[c] Chinese National Engineering Research Centre for Steel Construction (Hong Kong Branch),
the Hong Kong Polytechnic University, Hong Kong SAR, China.
[d] Department of Civil and Environmental Engineering, Imperial College London, UK.
[e] College of Civil Engineering and Architecture, Zhejiang University, Hangzhou, China.

Abstract

This paper investigates the structural behaviour of stud shear connections in composite floors with various connector arrangements and profiled deck configurations. The numerical investigation adopts a number of advanced finite element models which have been carefully calibrated against standard push-out tests conducted by the authors. In order to capture the complex interactions that take place between the concrete and the headed shear studs, a number of distinctive load transfer mechanisms within the solid concrete and the profiled composite slabs are identified and discussed. Detailed parametric studies are then undertaken using the calibrated models for the purpose of quantifying the shear resistance and deformation characteristics for connections with various stud and deck arrangements. A configuration parameter β is proposed for use in conjunction with the reduction factor k_t given in EN 1994-1-1 to incorporate the effects of installation positions of headed shear studs and trough widths of profiled decks as well as the presence of longitudinal stiffeners if any. It is shown that the values of β are in the range of 0.55 to 1.0, which are significantly smaller than those commonly allowed for in the design of stud shear connections in composite floors.

Keywords:
Stud shear connections; finite element modelling; load transfer mechanisms; load-slippage curves; shear resistances.

* *Corresponding author:* kwok-fai.chung@polyu.edu.hk

1. Introduction

In composite members, stud shear connectors of various forms are used to transmit longitudinal shear forces at the steel-concrete interfaces. The structural behaviour of these connectors has a direct influence on the effectiveness of the composite members in acting as integral members in resisting the applied loads. The most widely used shear connectors in building construction are headed shear studs, typically with a diameter of 19 mm, a height of 100 mm, and a tensile strength of 450 N/mm^2. Deformation characteristics of these stud shear connections in solid and composite slabs are commonly determined from push-out tests shown in Figure 1.

According to previous experimental investigations [1-3], numerical assessments [4-11], and theoretical studies [12, 13], the shear resistance of a stud shear connection in a composite beam with a profiled deck largely depends on the following factors:

a) concrete compressive and tensile strengths as well as elastic modulus;
b) tensile strength of headed shear studs as well as their shapes and sizes;
c) welding quality of shear studs and dimensions of welding collars at stud roots;
d) arrangements of headed shear studs within the troughs of profiled decks including position and spacing;
e) yield and tensile strengths of profiled decks and their cross-sectional shapes and dimensions, as well as sizes of longitudinal stiffeners in deck troughs, if present;
f) spanning direction of profiled decks, if present;
g) sizes and arrangement of steel reinforcement in the vicinity of the shear studs.

1.1 Recent experimental and numerical studies

Work carried out over the past decade have raised some concerns regarding the ductility of some forms of the stud shear connections for which considerable resistance degradation tend to occur at relatively small slippages [14]. However, in composite beams incorporating such shear connections, there was no apparent adverse effect on the overall beam behaviour, and their load-deflection curves were often shown to be sufficiently ductile [15]. Hence, there was a significant discrepancy in the deformation characteristics of these shear connections, as determined from push-out tests, when compared with those measured in beam tests. More recently, several researchers have also examined the shear resistances of these shear connections under combined shear and tension forces [16-18], as well as even under cyclic loading [19, 20]. In general, owing to the large number of factors that affect the structural behaviour of these stud shear connections, significant variations are often observed in the test results obtained from various push-out tests. It is therefore vital to select test results from only those experimental investigations which have been carefully and consistently executed, and which material data and test results have been presented in a systematic manner.

In recent years, several researchers have also investigated the fundamental behaviour of stud shear connections through advanced finite element modelling. Katwal et al [10] established a finite element model of a composite beam with a profiled deck by detailed modelling of the interaction between the steel beam and the composite slab. The stud shear force-slippage curves of the shear connections were obtained, and one of the key areas of investigation was to assess contributions of the profiled deck to the shear resistance of the connections. Vigneri et al. [11] also performed numerical simulations to identify various development stages of plastic hinges along the shanks of the headed shear studs. It is expected that such deformation characteristics would be more complex in composite beams with various connector arrangements and profiled deck configurations.

1.2 Experimental and numerical investigations by the authors

In order to assess and quantify the structural behaviour of stud shear connections in composite beams, an experimental assessment coupled with complementary numerical simulations was carried out previously by the authors [18, 21].

1.2.1 Systematic standard push-out tests

A total of three series of push-out tests comprising a total of 13 tests were undertaken to obtain the load-slippage curves of stud shear connections with different configurations, as shown in Figure 1:

- Test Series SS

  In this series, standard push-out tests were performed on stud shear connections with concrete solid slabs. Four pairs of headed shear studs were installed in each test specimen, and were fully embedded into the concrete. Both the measured load-slippage curves and the measured shear resistances of the test specimens are adopted as the reference data of the shear connections for subsequent comparisons.

- Test Series SCFr and SCUr

  In these two series, standard push-out tests were performed on shear connections in composite slabs. Four pairs of headed shear studs were employed in each test specimen, and were installed in either a “favourable” or an “unfavourable” position in the troughs of the profiled decks, owing to the presence of longitudinal stiffeners.

Among these tests, all specimens with solid concrete slabs failed through stud fracture while all specimens with composite slabs failed in concrete conical failure, as shown in Figure 2. The measured load-slippage curves were normalized through a linear reduction factor which is a ratio of the reference strength of 35 N/mm^2 to the measured compressive strength of the concrete, or of the reference strength of 500 N/mm^2 to the measured yield strength of the steel studs, depending on the modes of failure of the test specimens. Details of the material tests of both the concrete and the steel studs may be found in Shen [22].

Representative load-slippage curves of these shear connections with different configurations are plotted together for direct comparison, as shown in Figure 3, and the measured shear resistances per stud are summarized in Table 1 for ease of comparison. Based on the results of the push-out tests, a set of reduction factors allowing for the presence of the profiled decks as well as for different stud arrangements in the deck troughs have were obtained. It was found that the design rules for k_t given in EN 1994-1-1 [23] and BS 5950-3 [24] are inadequate for cases of headed shear studs installed in both the favourable and the unfavourable positions of the deck troughs.

It should be noted that a number of tensile tests were conducted on the coupons machined from the headed shear studs according to EN ISO 6892-1:2009 [25], and key mechanical properties obtained from measured engineering stress-strain curves of these studs were adopted for subsequent numerical analyses.

1.2.2 Development of advanced numerical models

Using detailed finite element procedures, material models and solution techniques [4-11], numerical simulations were carried out by the authors [21] to replicate the push-out tests described above. Element type C3D8R in ABAQUS [26] was used to model the concrete slab, the steel section and the headed shear studs while element S4R was adopted to model the deck. For the steel reinforcement, a two-noded linear three-dimensional truss element T3D2 was employed.

Key information of the finite element modelling technique is reported as follows.

a) Material model of stud steels

According to test results of standard tensile tests, the material model of the stud steels is represented with a non-linear true stress-strain relationship transformed by integration method based on the minimum engineering stress-strain curve. The deformation limit of true strain is specified as 5%. The transformation rules are:

$$\varepsilon_t = \ln(1+\varepsilon) \quad ; \text{and}$$

$$\sigma_t = \sigma(1+\varepsilon)$$

where

σ and ε are the engineering stress and strain, respectively, and

σ_t and ε_t are the true stress and strain, respectively.

Since the objective of the present study is to investigate the load-transfer mechanisms of the shear connections, the deformation limit of 5% in the shear studs defined in the material model is considered to be sufficient to identify all possible failure modes in the shear connections.

b) Material models of concrete

For the concrete material, the concrete damaged plasticity (CDP) model [27-29] is adopted which involves two main failure mechanisms, namely, i) compressive crushing, and ii) tensile cracking. In general, this model assumes that the uni-axial compressive and tensile response of the concrete is characterized by damaged plasticity, and this simplified representation is able to capture main features of the mechanical responses of the concrete readily. The yield function of this model is proposed by Lubliner et al. [28], and then subsequently modified by Lee et al. [29]. In the present numerical investigation, the following values of the plasticity parameters of the concrete are adopted for the CDP model in ABAQUS [26]:

i) Ψ is the dilation angle measured on the p-q plane at high confining pressures, and it is taken to be 40°;

ii) M is a parameter that defines the rate at which the function approaches the asymptote, and it is taken to 0.1;

iii) f_{b0}/f_{c0} is a ratio of the initial bi-axial compressive yield stress to the initial uni-axial compressive yield stress, and it is taken as 1.16;

iv) K_c is a ratio of the second stress invariant on the tensile meridian, q(TM), to that on the compressive meridian, q(CM); and it is taken to be 0.667;

The viscosity parameter is taken to be zero so that no visco-plastic regularization is performed. For further details on the values of those parameters, refer to Qureshi et al. [5]. In general, the model is shown to give good predictions when the concrete is under uni-axial and bi-axial stress states. It should also be noted that:

- under uni-axial compression, the stress-strain relationship provided by EN 1992-1-1 [30] and the elastic modulus of the concrete given in the Hong Kong Concrete Code [31] are adopted; and
- under uni-axial tension, the tensile behaviour of the concrete is interpreted as the relationship between the tensile stress and the cracking displacement given in both EN 1992-1-1 [30] and fib Model Code 2010 [32].

It should be noted that a new CDP model with mesh-insensitivity proposed by Alfarah et al [27] is reported to be very effective in modelling concrete cracking, concrete crushing, and reinforcement steel yielding in typical reinforced concrete members under both monotonic and cyclic actions.

a) Contact models

In order to model the surface-to-surface contact in the shear connections properly, the following four models of contact pairs are set up:

i) the steel section onto the concrete slab,
ii) the headed shear stud onto the concrete,
iii) the top surface of the profiled deck onto the concrete, and
iv) the bottom surface of the profiled deck onto the steel sections.

In general, the properties of the surface-to-surface contact include:

- for the normal behaviour, a hard contact is assumed in all interaction surfaces to minimize any penetration of a slave surface to a master surface, and no transfer of tensile stress across the interface is allowed; and
- for the tangential behaviour, a penalty friction formulation with a friction coefficient of 0.5 is used for all the surface-to-surface contact, except for the steel-deck contact pair which is assumed to be frictionless.

b) Qusi-static analysis with the dynamic/explicit method

In order to incorporate the complex contact conditions in the stud shear connections, and to model concrete crushing and cracking effectively, the quasi-static analysis with the dynamic/explicit method in the ABAQUS is adopted. Both numerical accuracy and computational efficiency of the finite element models are ensured with an introduction of a mass scaling as follows:

- The mass scaling factors of 1500, 1000, 500, 50 have been applied to the models, and the ratios of kinetic energy to internal energy (ALLKE/ALLIE) are monitored. A mass scaling of 500 is found to be appropriate while the value of ALLKE/ALLIE is found to be less than 1%.

- The loading is applied in the form of a displacement control, and the development of the loading rate is defined with a smooth step function. This function is intended to smoothly ramp up the rate of loading application from zero to a specified magnitude over a short specified period of time The loading rate is then kept constant for the rest of the analyses. The purpose of this loading method is to keep the magnitude of the kinetic energy at a very low level. Various loading rates of 5, 0.5, 0.05, and 0.01 mm/sec have been applied to the models in a sensitivity study. Based on the results of the study, a loading rate of 0.05 mm/sec is adopted for all subsequent analyses.

c) Finite element analyses and convergence study

Typical finite element models for these shear connections are illustrated in Figure 4. Three shear connections with different configurations, as shown in Figure 5, have been successfully calibrated with the test results, noting that the names of the models are similar to those of the push-out tests.

A convergence study was carried out on finite element meshes with the concrete and the headed shear studs of different element sizes [22]. It should be noted that the most critical regions are often the shank roots of the headed shear studs and their surrounding concrete, and hence, these regions are systematically refined with reduced mesh sizes locally. After a convergence study with various mesh sizes of 15.0, 7.5, and 4.0 mm for the concrete, and of 12.0, 6.0, and 3.0 mm for the headed shear studs as shown in Figure 6, the key results are presented in Table 2. It is shown that a mesh size of 7.5 mm for the concrete and a mesh size of 6.0 mm for the shear studs are shown to be both structural accurate and computationally efficient, and hence, these element sizes were adopted for subsequent numerical investigations. Figure 5 plots both the measured and the predicted load-slippage curves of Models SS, SCFr, and SCUr onto the same graph for easy comparison, and both measured material and geometrical properties were adopted in the models. It is shown that the predicted curves of the three models were found to be very close to those obtained from the push-out tests.

This excellent comparison provides confidence in the accuracy of the advanced finite element models for these shear connections. Hence, the models can be used to predict with a high level of reliability the deformation characteristics of various types of stud shear connections, including capturing concrete crushing and cracking as well as shear yielding of headed shear studs. These numerical models are adopted in the present investigation for detailed assessments and parametric studies.

1.3 Shear resistances of shear connections in solid and composite slabs

Design methods for the shear resistances of stud shear connections with solid concrete slabs in several current codes of practice are based on the research work of Ollgaard et al. [33]. For example, in Cl. 6.6.3.1 of EN 1994-1-1 [23], the design shear resistance of a shear connection with headed shear studs fully embedded inside a solid concrete slab, Q_{SS} , is given by the smaller of the two values obtained from the following equations:

$$Q_{m,CF} = 0.29 d^2 \sqrt{f_{ck} E_{cm}} \times \frac{1}{\gamma_V} \tag{1a}$$

or

$$Q_{m,\mathrm{SF}} = 0.8 f_u \left(\frac{\pi d^2}{4} \right) \times \frac{1}{\gamma_V} \tag{1b}$$

where f_{ck} is the characteristic cylinder compressive strength of the concrete; E_{cm} is the mean elastic modulus of the concrete; d is the diameter of the stud shank; f_u is the tensile strength of the stud shank, and γ_V is the partial factor with a recommended value of 1.25.

It should be noted that Equation (1a) relates to failure of the concrete while Equation (1b) relates to a shear failure of the steel stud [4]. According to Cl. 6.6.4.2 of EN 1994-1-1 [23], an additional shape factor, k_t , is introduced to the design shear resistance of the shear connection, Q_{SS} , to allow for the presence of the profiled decks which are perpendicular to supporting steel beams as follows:

$$k_t = \frac{0.7}{\sqrt{n_r}} \frac{b_o}{h_p} \left(\frac{h}{h_p} - 1 \right) \qquad (2)$$

where n_r is the number of shear stud(s) per trough; h and d are the height and the diameter of the shear stud, respectively; and h_p and b_o are the depth and the average width of the deck trough, respectively. It should also be noted that b_o is the average trough width for trapezoidal profiled decks, and is the minimum trough width for re-entrant profiled decks.

As various forms of profiled decks typically have longitudinal stiffeners in their troughs to improve their moment resistances, there are two different positions for the shear studs to be installed in the deck troughs, namely: i) a favourable position, and ii) an unfavourable position, as shown in Figure 1. It should be noted that these two positions in the deck troughs are classified according to different support and loading conditions of the composite floors. Various studies [2, 3, 5-8] have shown that there are significant differences in the deformation characteristics of composite beams with shear studs installed at different positions of the deck troughs. Hence, there is a need to develop design rules to assess the effects of installation positions of these shear studs in composite beams with profiled decks.

2. Objectives and Scope of Work

In order to examine the structural behaviour of stud shear connections in composite floors with various stud arrangements and profiled deck configurations, the validated finite element models, reported in Section 1.2 above, are employed herein in a detailed numerical investigation. A number of finite element models for typical shear connections in those composite beams with profiled decks spanning perpendicular to supporting steel beams are constructed, and a detailed assessment is conducted in order to identify various load transfer mechanisms. Moreover, parametric studies are performed with various stud arrangements and profiled deck configurations to assess the deformation characteristics of these shear connections.

It should be noted that the structural behavior of such shear connections is complex, and depends on several inter-independent parameters. It cannot, therefore, be adequately and practically quantified within an experimental assessment. To ensure that the numerical assessment provides information that enables focused quantification of the influence of key parameters, the following two main tasks were identified:

i) Task A Load transfer mechanism

A total of four finite element models of the stud shear connections with profiled decks were constructed, and non-linear analyses were performed in order to examine the "stress and strain" conditions of these connections at large deformations, based on which specific load transfer mechanisms within the shear connections can be identified and assessed; and

ii) Task B Parametric studies

A total of 16 finite element models of the stud shear connections were constructed and used to for parameter variations including the concrete cube strength, stud arrangements and profiled deck configurations, with a particular focus on their influence on the connection resistances.

It should be noted that in these parametric studies, a profiled deck of 1.0 mm thick and a yield strength of 280 N/mm^2 was used; headed shear studs of a shank diameter of 19 mm and a welded height at 95 mm were adopted; the tensile strength of the shear studs after cold forging was assumed as 450 N/mm^2; the height and the diameter of welding collars of headed shear studs were assumed to be 3 and 25 mm respectively; and pairs of headed shear studs were installed at a transverse spacing of 100 mm.

The key areas of interest of the numerical investigations include:

i) internal force distributions within various shear connections, and their corresponding load transfer mechanisms;

ii) typical failure modes of the shear connections with various stud arrangements and profiled deck configurations; and

iii) effects of longitudinal stiffeners in the deck troughs on the deformation characteristics of the shear connections.

Based on the results of the detailed numerical investigations, a configuration parameter, β , is proposed to allow for any reduction in the shear resistance of the connections due to the effects of various stud arrangements and profiled deck configurations.

It should be noted that after successful completion of these numerical investigations, it is possible to examine structural behaviour of shear connections with different combinations of stud arrangements in the deck troughs, for example, staggered or alternate arrangements of studs in either "favourable" or "unfavourable" positions.

3. Load Transfer Mechanisms

The position of the shear studs in the deck troughs (i.e. favourable or unfavourable) has a direct effect on the connection behaviour in the push-out tests. In order to quantify the structural behaviour of these stud shear connections with various stud arrangements and profiled deck configurations, the following four models are established:

- Model SS is established to model typical shear connections with solid concrete slabs, and it is a reference model for comparison with the other three models with profiled decks.

- Model SC represents typical shear connections in composite beams with profiled deck in which the shear studs are installed at the centers of the deck troughs.

- Models SCFr and SCUr are variants of Model SC, in which the shear studs are installed at the favourable and the unfavourable positions in the deck troughs, respectively.

It should be noted that Models SS, SCFr and SCUr have been directly calibrated against test results as described in Section 1.2. However, no calibration for Model SC against test data is possible owing to the presence of longitudinal stiffeners at the centers of the deck troughs, and hence, headed shear studs cannot be physically installed at the centers of the deck troughs.

3.1 Numerical results

The four models provided detailed results which were used to examine the failure conditions. For each model, the following results are extracted: i) a two-dimensional deformed mesh showing deformations of the shear studs, and highly localized areas in terms of concrete stresses, and ii) a simplified force diagram of the connection. It should be noted that F_v, F_c and M are the internal shear force, the internal tension force and the local moment at the root of the headed shear stud, respectively; while F_{fict} is the total frictional force of the shear connection between the concrete and the top surface of the steel flange or the profiled deck. The numerical results for all four models are presented collectively together in Figure 7 for direct comparison. Moreover, in order to present clear illustrations of damaged concrete in these models, three-dimensional images of concrete crushing and cracking are also provided, related to which the following definitions of concrete failure are adopted:

i) a concrete crushing zone is identified in term of a compressive equivalent plastic strain, PEEQ [26], and it is assumed that those concrete elements with a PEEQ value exceeding 0.005 have crushed [21, 22]; and

ii) a concrete cracking damage is considered in term of a cracking displacement using a function of DAMAGET [26], and it is assumed that concrete elements with a DAMAGET reaching a value of 1.0 have cracked.

Both the cracking and the crushing zones of the damaged concrete in the four models are highlighted in different colors in Figure 7. It is shown that:

a) In Model SS, the applied loads are transferred from the steel section to the concrete slabs through the shear studs, i.e. through *shear action*, which are in turn transferred onto the surrounding concrete through *local bearing*. These *bearing forces* are readily built up at the roots of the studs where many concrete elements are highly stressed under compression; the bearing forces diminish quickly as they move away from the steel-concrete interface. As there are many concrete elements available in the concrete slab to receive the *applied forces*, a conical concrete failure over a large area of concrete is unlikely to take place. Instead, the connection typically fails in stud shear failure at a large deformation beyond 6 mm.

b) In Model SC, the applied loads are transferred from the steel section to the composite slab, i.e. the continuous portion of the concrete slab, through the shear studs. These *shear forces* are in turn transferred onto the surrounding concrete through *local bearing* acting on the shear studs. The *bearing forces* are readily built up at the roots of the studs though they diminish quickly once they move away from the steel-concrete interface. Owing to the presence of the profiled deck, or more precisely, an absence of the corresponding concrete elements, there are only limited concrete elements behind the shear studs, and hence, the load transfer from these 'trough' concrete onto the 'slab' concrete may become critical. Hence, a conical concrete failure over the 'slab' concrete in the shear connection is often critical, and the corresponding shear resistance of the shear connection is significantly reduced, when compared with that of Model SS. Moreover, as all these forces act eccentrically to the 'slab' concrete, local moments are induced, and many elements in the continuous portion of the slab are cracked.

c) Similar to the load path established in Model SC, the applied loads in both Models SCFr and SCUr are shown to be readily transferred from the steel sections to the continuous portions of the composite slabs through the shear studs. These *shear forces* are transferred from the shear studs onto the surrounding concrete through *local bearing*. However, depending on the amount of the 'trough' concrete receiving these bearing forces, there are two different mechanisms:
   - In Model SCFr, owing to the presence of a relatively large lump of 'stiff and strong' concrete in the 'trough' behind the shear studs, it receives the bearing forces readily as compressive forces, and transfers them into shear forces acting onto the continuous portion of the composite slab without causing any significant deformation in the stud. At the same time, this lump of "trough" concrete is subjected to
     i) the bearing forces acting close to the shank roots of the studs, and
     ii) the reaction forces acting along the continuous portion of the concrete slab.

Hence, this lump of "trough" concrete together with neighbouring "slab" concrete is under a large local moment, and they tend to rotate as a whole. As the applied shear forces increase in magnitude, a conical failure will take place in the "slab" concrete under the action of the tension forces induced by the moments. It should be noted that this is a non-ductile mode of failure.

- In Model SCUr, there is only a small lump of "trough" concrete behind the shear studs which is not stiff nor strong enough to receive the applied forces, and hence, this "trough" concrete is unable to provide an effective load path, i.e. from bearing forces to compressive forces, to transfer the applied forces to the continuous portion of the composite slab. Instead, the studs receive the applied forces directly at their shank roots while their shanks deform readily into a double curvature under shear action, i.e. a dowel mechanism, to transfer the applied forces while most of the neighbouring "trough" concrete is cracked. In general, this is a highly ductile mode because of the dowel mechanism of the shear studs.

For ease of presentation, ductility of the stud shear connections is classified as follows:

- highly ductile when $s_u \geq$ 5.5 mm, and s_u - s_m = 3.5 ~ 4.5 mm
- ductile when s_u = 4.5 ~ 5.5 mm; and s_u - s_m = 2.5 ~ 3.5 mm
- non-ductile when $s_u \leq$ 4.5 mm, and s_u - s_m = 1.0 ~ 2.5 mm

where
s_m is the slippage corresponding to Q_m; and
s_u is the slippage corresponding to 0.8 Q_m (unloading).

3.2 Load paths within connections

In order to provide an overall understanding of various load transfer mechanisms within the shear connections, simplified load paths of all the four models are illustrated in Figure 8. In general, the structural behaviour of Model SS (i.e. the stud shear connections with solid concrete slabs) depends primarily on the highly compressed concrete behind the shear studs. As these concrete areas are relatively stiff and strong, only local concrete crushing takes place, and the critical failure mode of the connection is shear-off failure of the steel stud.

For those shear connections with various stud arrangements and profiled deck configurations, various parts and extents of the concrete are cracked and crushed, as shown in Figure 8, depending on their different positions in the deck troughs. They may be broadly classified as:

i) Large concrete behind shear studs with a non-ductile failure
   In Model SCFr, large "trough" concrete are 'stiff and strong', and they are able to stand the bearing forces from the shear studs. These forces are readily received by the 'trough' concrete as compression forces, and then transferred onto the 'slab' concrete through shear action. Essentially, the load path goes through the "trough" concrete, and a non-ductile conical shear failure of the concrete is often critical.

ii) Sufficient concrete behind shear studs with a ductile failure
   In Model SC, the "trough" concrete is sufficiently effective to transfer compression forces, when compared with that in Model SCFr. Moreover, the dowel mechanism is effective to maintain the shear resistances under a limited slippage. Essentially, the load path goes through the "trough" concrete, and a conical failure in the concrete often becomes critical at large deformations.

iii) Small concrete behind shear studs with a highly ductile failure
   In Model SCUr, the 'trough' concrete is unable to transfer compression forces effectively. Instead, the applied forces are transferred through a dowel mechanism of the shear studs, i.e. the stud shanks are bent into a double curvature so that the applied forces are transferred into the 'slab' concrete through the embedded heads of the shear studs. Essentially, the load path goes through the shear studs, which fail under combined shear and bending in a highly ductile manner.

For detailed discussions on both the forces and the moments along the lengths of the headed shear studs within these connections, refer to References 21 and 22.

4. Parametric Assessments

In order to generate design data for assessing the shear resistance of the stud shear connections with various stud arrangements and profiled deck configurations, detailed parametric studies were undertaken using the validated finite element models presented above. Key parameters considered include:

- Installation positions of shear studs

  For each connection, the shear studs are installed at one of the three positions of the deck troughs, namely:

  i) central position, denoted as “C”,

  ii) favourable position, denoted as “F”, and

  iii) unfavourable position, denoted as “U”.

- Configuration of profiled decks

  For each connection, the trough widths of the deck, b_o, are assigned as 110, 135 or 160 mm, while the deck height is assumed to be 50 mm in all cases. In the presence of longitudinal stiffeners in the central positions of the deck troughs, their height is considered as 10 mm in all cases, and this is denoted as “r’.

Figure 9 depicts a total of 16 finite element models established for the present parametric studies, and Table 3 summarizes the programme of the parametric studies together with key results. It should be noted that all the numerical results provided above are based on a tensile strength of 450 N/mm^2 for the stud steel, and a cube strength of 30 N/mm^2 for the concrete material. Comparative assessments of the numerical results are presented below.

4.1 Study PS01

In this study, the shear resistances of the stud shear connections with installation positions at C, F and U, and trough width b_o = 160, 135, and 110 mm, are compared as follows:

a) Model SS results in high strength and ductility; a shear resistance of 105.1 kN per stud is attained, i.e. Q_{SS} = 105.1 kN. The load-slippage curve is depicted in various graphs, as shown in Figure 10, and considered as the reference curve for comparison.

b) All the deformation characteristics of various groups of these shear connections are plotted in the same graphs in Figure 10 for direct comparison. It is shown that all load-slippage curves of Models SC-C (with various trough widths) may be regarded as ductile, while those of Models SC-F and SC-U are considered to be non-ductile and highly ductile respectively.

c) In the presence of the profiled deck with trough widths of 160, 135 and 110 mm, significant reduction in the shear resistances of the connections occurs. In general, the reduction factors for Models SC-160F, -135F and -110F are found to be 0.80, 0.75 and 0.65, respectively. For Models SC-160C, SC-135C and SC-110C, the corresponding reduction factors are found to be 0.73, 0.69 and 0.62 respectively. For Models SC160-U, SC-135U and SC-110U, the corresponding reduction factors are found to be 0.75, 0.68 and 0.62 respectively.

d) Accordingly, when the shear studs are installed at the favourable positions in the deck troughs, instead of the central positions, the corresponding reduction factors are increased by values of 0.06 to 0.07 when b_o = 160 or 135 mm.

4.2 Study PS02

In this study, the shear resistances of the stud shear connections with installation positions at C, F & Fr, and U & Ur, and trough width b_o = 160, 135, and 110 mm are compared. The deformation characteristics of various model groups are plotted in the same graphs for direct comparison in Figures 11, 12 and 13, and these deformation characteristics are shown to be very similar among those stud shear connections with the same installation positions, as discussed in the section above. It is shown that:

a) Model SS results in high strength and ductility; a shear resistance of 105.1 kN per stud is attained, i.e. Q_{SS} = 105.1 kN. The load-slippage curve is used as the reference curve. Similarly, the load-slippage curves of Models SC-110C, SC-135C, and SC-160C are also adopted as basic curves for subsequent comparisons with shear connections with various stud arrangements and profiled deck configurations. It should be noted that their shear resistances are found to be 0.62, 0.69, and 0.73 Q_{SS} respectively.

b) When the headed shear studs are installed at the favourable positions in the deck troughs, i.e. Models SC-160F, SC-135F, and SC-110F, the shear resistances of the shear connections are 0.80, 0.75, and 0.65 Q_{SS}. However, in the presence of longitudinal stiffeners in the deck troughs, i.e. Models SC-160Fr, SC-135Fr, and SC-110Fr, the shear resistances of the shear connections are further reduced to 0.74, 0.68, and 0.58 Q_{SS} respectively. Both load-slippage curves are considered non-ductile.

c) When the headed shear studs are installed in the unfavourable positions in the troughs of the deck, i.e. Models SC-160U, SC-135U, and SC-110U, the shear resistances of the shear connections are found to be 0.75, 0.68, and 0.62 Q_{SS}. In the presence of longitudinal stiffeners in the troughs of the deck, i.e. Models SC-160Ur, SC-135Ur, and SC-110Ur, the shear resistances of the connections are further reduced to 0.58, 0.50, and 0.42 Q_{SS}. However, the load-slippage curves are highly ductile.

The equivalent compressive plastic strains, PEEQ, in the concrete slabs of various models are also illustrated in Figures 11, 12, and 13 for direct comparison. In general, their patterns in the stud shear connections with various connector arrangements and profiled deck configurations are shown to be very similar.

4.3 Shear resistances of stud shear connections

In order to provide data on the shear resistances of these stud shear connections with various concrete grades, an extensive set of 80 analyses was carried out with concrete compressive strengths ranging from 30 N/mm^2 to 50 N/mm^2. The predicted shear resistances per stud for connections with various groups of stud arrangements and profiled deck configurations are plotted in the same graphs for direct comparison, as shown in Figures 14, 15 and 16. It is shown in the figures that:

- By increasing the concrete cube strengths f_{cu} from 30 to 50 N/mm^2, the shear resistance of the stud shear connections, for various arrangements, increases slightly.

- The installation positions of the studs in the profiled deck are very important, and the presence of a sufficiently large concrete area behind the shear studs increases the shear resistances of the shear connections.
- By reducing the trough widths b_o from 160 to 110 mm, the shear resistance of the connections decreases slightly.
- The presence of longitudinal stiffeners in the deck troughs reduces the shear resistances of the connections significantly when the shear studs are installed in the unfavourable positions in the deck troughs.

In order to capture the influence of stud arrangements and profiled deck configurations, a configuration parameter β is proposed in conjunction with the reduction factor k_t. The suggested design approach is therefore given as follows:

$$Q_m \quad = \quad \beta \times k_t \times \min\{ Q_{m,CF}, Q_{m,SF} \} \qquad (3)$$

where: $Q_{m,CF}$ and $Q_{m,CF}$ are given by Equations (1a) and (1b) with the partial factor γ_v equal to 1.0, k_t is the reduction factor given by Equation (2); and β is a configuration factor proposed in this study based on the results of the parametric studies, with the values of β as given in Table 4.

In general, the values of β depend on the geometry as well as the dimensions of the profiled deck, including the heights and widths of the troughs, and the heights of the longitudinal stiffeners, if any. It should be noted that:

i) for shear connections with profiled deck with b_o at 160 mm, the values of β range from 1.00 to 0.75.

ii) for shear connections with profiled deck with b_o at 135 mm, the values of β range from 0.95 to 0.65; and

iii) for shear connections with profiled deck with b_o at 110 mm, the values of β range from 0.85 to 0.55.

5. Conclusions

This paper presents a detailed study into the structural behaviour of stud shear connections with various commonly used stud arrangements and profiled deck configurations. In order to examine and quantify the behaviour, a detailed numerical investigation is carried out followed by a parametric assessment covering a wide range of practical shear connections with both solid concrete slabs and composite slabs. The main findings of the study can be summarized as follows:

a) Based on the numerical results of the experimentally validated and calibrated finite element models, the detailed stress distributions of various stud shear connections were used in order to identify the underlying load transfer mechanisms. Simplified load paths within these models were also highlighted by considering the 'stress and strain' plots of the models at failure, and three dimensional plots of the damaged concrete. It was shown that the effectiveness of the 'trough' concrete in resisting the applied loads, and then transferring them to the 'slab' concrete is vital in determining the structural behaviour of these stud shear connections. When there are sufficiently large concrete areas behind the shear studs, the connection exhibits a relatively high shear resistance, but a non-ductile load-slippage curve. In contrast, when there is only limited concrete behind the shear studs, the connection has a relatively low shear resistance but a highly ductile load-slippage curve as it is the shear studs that determine the ultimate behaviour.

b) The results of parametric studies on the shear connections, with various stud arrangements and profiled deck configurations, enable a comparison of the load-slippage curves and shear resistances against those of shear connections with solid concrete slabs. It is shown that shear connections with solid concrete slabs consistently offer high strength and ductility. However, in the presence of profiled decks, the load-slippage curves of those connections with shear studs installed at the favourable or the unfavourable positions are very different. The load-slippage behaviour of Model SS is considered to be highly ductile while that of Model SC is considered to be ductile. On the other hand, Models SC-F and SC-U result in a non-ductile and a highly ductile response, respectively.

c) In order to assess the effects of stud arrangements and profiled deck configurations on the shear resistances of the shear connections, a total of 80 finite element analyses were performed. A configuration parameter β is proposed, based on the results of these analyses, to be used in conjunction with the reduction factor k_t adopted in EN 1994-1-1. It should be noted that the values of β are found numerically to range from 0.55 to 1.0 for various installation positions of headed shear studs, trough widths of the profiled decks, and the presence of longitudinal stiffeners, if any.

Overall, this paper provides detailed insights into the structural behaviour of the stud shear connections including the load transfer mechanisms. This investigation also quantifies the reduction in the shear resistances of these shear connections with various stud arrangements and profiled deck configurations. The effects of these reductions are considerably more pronounced than those commonly allowed for in the design of stud shear connections in composite structures, and point to the need for modification of current codified procedures.

Acknowledgements

The research project leading to publication of this paper is funded by the Research Grants Council of the University Grants Committee of the Government of Hong Kong SAR (Project No. PolyU 5143/13E), and the Chinese National Engineering Research Centre for Steel Construction (Hong Kong Branch) funded by the Innovation and Technology Commission of the Government of Hong Kong SAR, and the Research Committee of the Hong Kong Polytechnic University. The research work reported in this paper is part of the research study of the first author at The Hong Kong Polytechnic University. Moreover, the supply and fabrication of the steel sections of the test specimens by Wo Lee Steel Co. Ltd., Genyield Construction Co. Ltd., and STAM Steel Co. Ltd. are gratefully acknowledged.

References

[1] D.J. Oehlers, R.P. Johnson. The strength of stud shear connections in composite beams. The Structural Engineer. 65 (1987), 44-48.

[2] J.T. Mottram, R.P. Johnson. Push tests on studs welded through profiled steel sheeting. University of Warwick1989.

[3] R.P. Johnson, H. Yuan. Existing rules and new tests for stud shear connectors in troughs of profiled sheeting. P I CIVIL ENG-STR B. 128 (1998), 244-251.

[4] D. Lam, E. El-Lobody. Behavior of headed stud shear connectors in composite beam. J STRUCT ENG. 131 (2005), 96-107.

[5] J. Qureshi, D. Lam, J. Ye. Effect of shear connector spacing and layout on the shear connector capacity in composite beams. J CONSTR STEEL RES. 67 (2011), 706-719.

[6] J. Qureshi, D. Lam, J. Ye. The influence of profiled sheeting thickness and shear connector’s position on strength and ductility of headed shear connector. ENG STRUCT. 33 (2011), 1643-1656.

[7] E. Ellobody, B. Young. Performance of shear connection in composite beams with profiled steel sheeting. J CONSTR STEEL RES. 62 (2006), 682-694.

[8] J. Qureshi, D. Lam. Behaviour of headed shear stud in composite beams with profiled metal decking. ADV STRUCT ENG. 15 (2012), 1547-1558.

[9] F. Tahmasebinia, G. Ranzi, A. Zona. Probabilistic three-dimensional finite element study on composite beams with steel trapezoidal decking. J CONSTR STEEL RES. 80 (2013), 394-411.

[10] U. Katwal, Z. Tao, M.K. Hassan. Finite element modelling of steel-concrete composite beams with profiled steel sheeting. J CONSTR STEEL RES. 146 (2018), 1-15.

[11] V. Vigneri, C. Odenbreit, M. Braun. Numerical evaluation of the plastic hinges developed in headed stud shear connectors in composite beams with profiled steel sheeting. Structures (2019).

[12] D.J. Oehlers, M.A. Bradford. Composite steel and concrete structural members: fundamental behaviour. Oxford: Pergamon Press1995.

[13] R.P. Johnson, R.J. Buckby. Composite Structures of Steel and Concrete. Wiley Online Library1975.

[14] S. Hicks. Strength and ductility of headed stud connectors welded in modern profiled sheeting. Structural Engineer. 85 (2007), 32-39.

[15] G. Ranzi, M.A. Bradford, P. Ansourian, A. Filonov, K. Rasmussen, T.J. Hogan, B. Uy. Full-scale tests on composite steel – concrete beams with steel trapezoidal decking. J CONSTR STEEL RES. 65 (2009), 1490-1506.

[16] O. Mirza, B. Uy. Effects of the combination of axial and shear loading on the behaviour of headed stud steel anchors. ENG STRUCT. 32 (2010), 93-105.

[17] Z. Lin, Y. Liu, J. He. Behavior of stud connectors under combined shear and tension loads. ENG STRUCT. 81 (2014), 362-376.

[18] M.H. Shen, K.F. Chung. Experimental investigation into stud shear connections under combined shear and tension forces. J CONSTR STEEL RES. 133 (2017), 434-447.

[19] Q. Sun, X. Nie, M.D. Denavit, J. Fan, W. Liu. Monotonic and cyclic behavior of headed steel stud anchors welded through profiled steel deck. J CONSTR STEEL RES. 157 (2019), 121-131.

[20] B. Lu, C. Zhai, S. Li, W. Wen. Predicting ultimate shear capacities of shear connectors under monotonic and cyclic loadings. THIN WALL STRUCT. 141 (2019), 47-61.

[21] M.H. Shen, K.F. Chung. Structural behaviour of stud shear connections with solid and composite slabs under co-existing shear and tension forces. Structures. 9 (2017), 79-90.

[22] M.H. Shen. Structural behavior of shear connections in composite structures under complex loading conditions. PhD thesis. The Hong Kong Polytechnic University (2013).

[23] BSI. BS EN 1994-1-1: 2004. Eurocode 4: Design of Composite Steel and Concrete Structures. Part 1-1: General rules and rules for buildings. British Standards Institution (2004).

[24] BSI. BS 5950: Structural Use of Steelwork in Building. Part 3 Section 3.1: Code of Practice for Design of Composite Beams. British Standards Institution (1990).

[25] BSI. BS EN ISO 6892-1: Metallic materials – Tensile testing. Part 1: Method of test at ambient temperature. British Standards Institution (2009).

[26] Abaqus. Abaqus User's Manual, Version 6.14. Dassault Systemes Simulia Corp.2014.

[27] B. Alfarah, F. López-Almansa, S. Oller. New methodology for calculating damage variables evolution in Plastic Damage Model for RC structures. ENG STRUCT. 132 (2017), 70-86.

[28] J. Lubliner, J. Oliver, S. Oller, E. Oñate. A plastic-damage model for concrete. INT J SOLIDS STRUCT. 25 (1989), 299-326.

[29] J. Lee, G.L. Fenves. Plastic-damage model for cyclic loading of concrete structures. J ENG MECH. 124 (1998), 892-900.

[30] BSI. BS EN 1992-1-1: 2004. Eurocode 2: Design of Concrete Structures. Part 1-1: General rules and rules for buildings. British Standards Institution (2004).

[31] BD. Code of Practice for the Structural Use of Concrete. Buildings Department of the Government of Hong Kong (2004).

[32] CEB. CEB-FIP Model Code. Comité Euro-International du Béton, Thomas Telford, London (2010).

[33] J.G. Ollgaard, R.G. Slutter, J.W. Fisher. Shear strength of stud connectors in lightweight and normal weight concrete. Engineering Journal-American Institute of Steel Construction (1971).

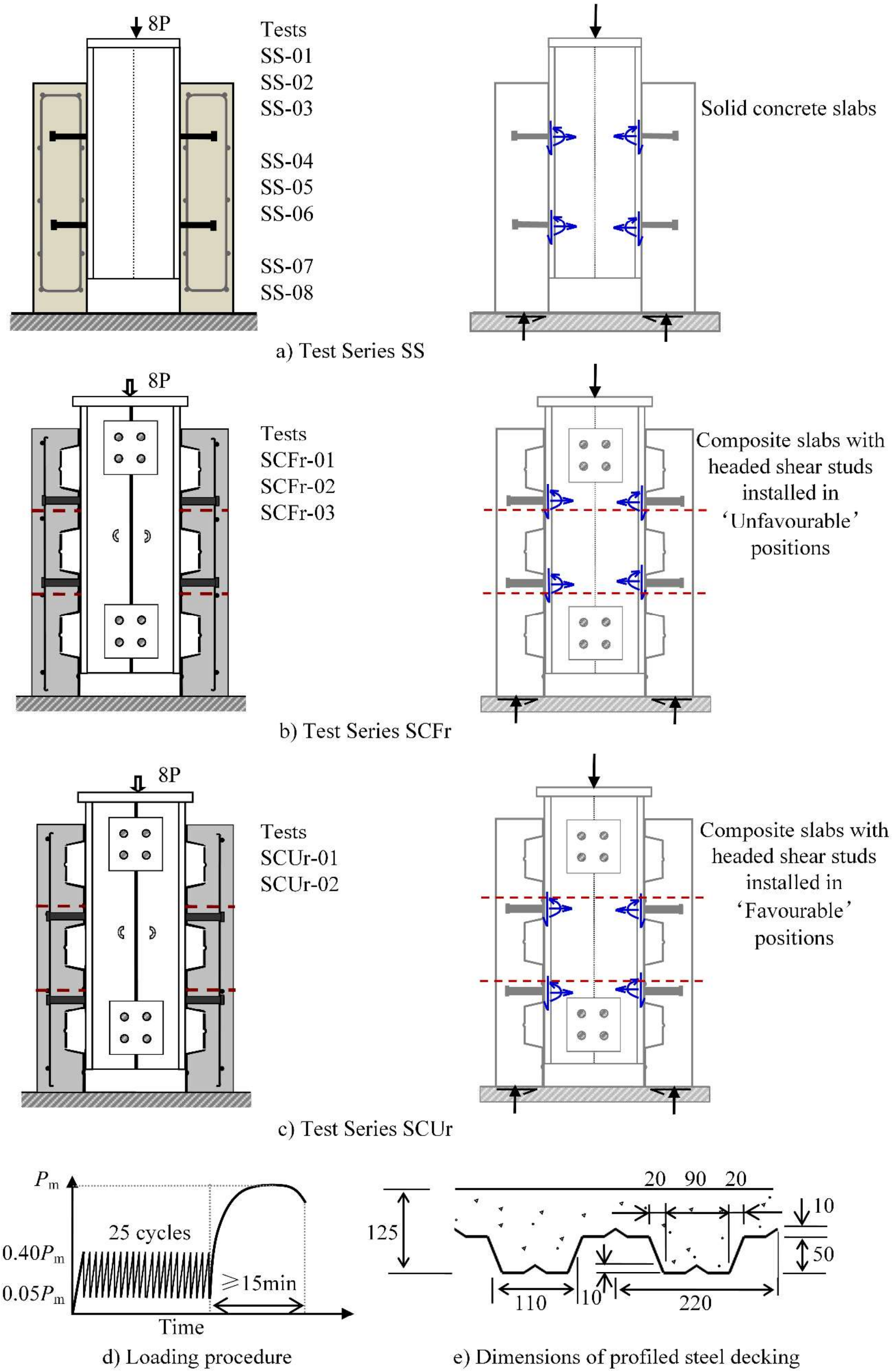

Figure 1: Push-out tests conducted by Shen and Chung [18]

Figure 2: Typical concrete conical failure in shear connections with composite slabs

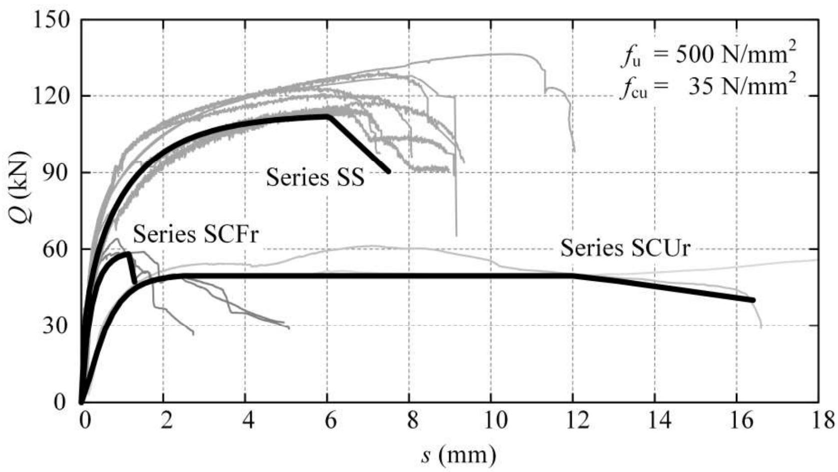

Figure 3: Standardized load-slippage curves of push-out tests

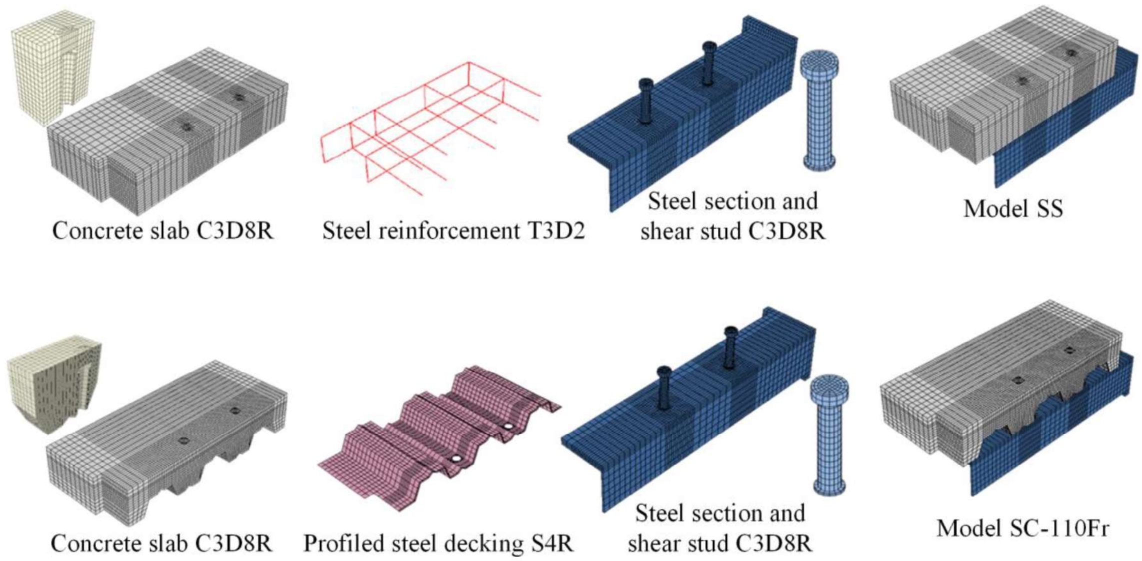

Figure 4: Finite element modelling

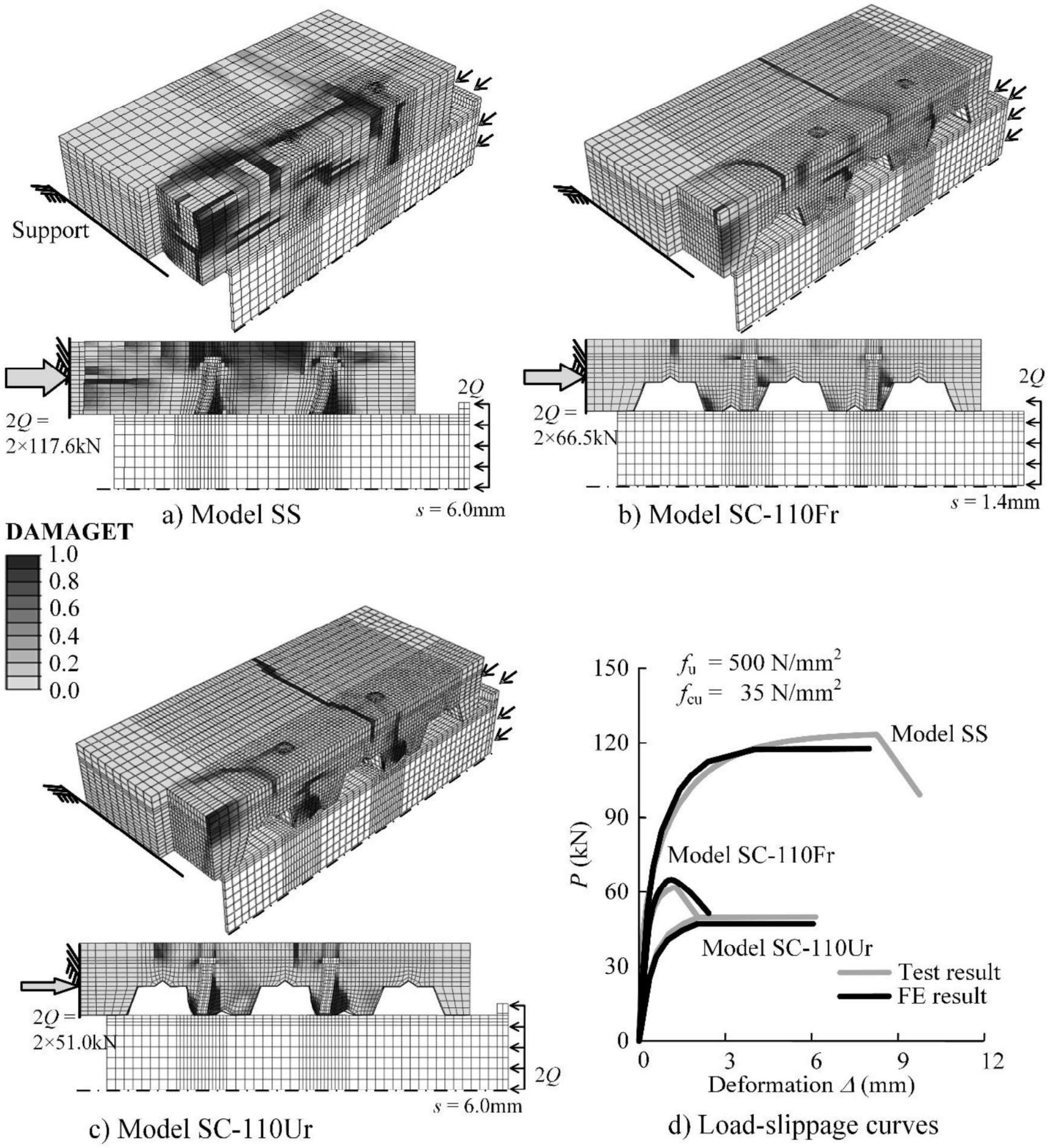

Figure 5: Numerical results of Models SS and SC

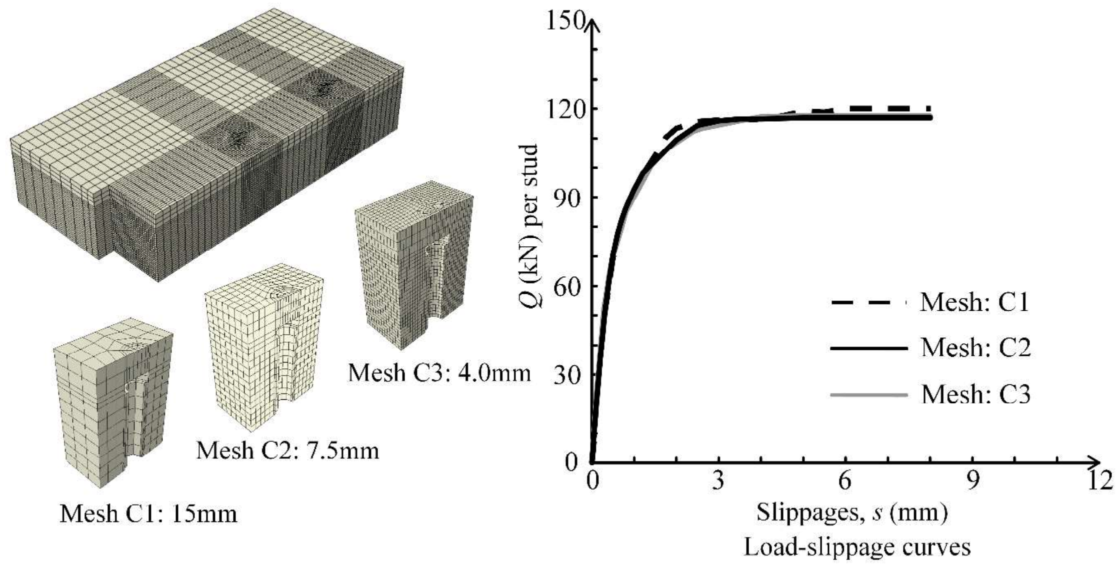

a) Various mesh sizes of the concrete slabs

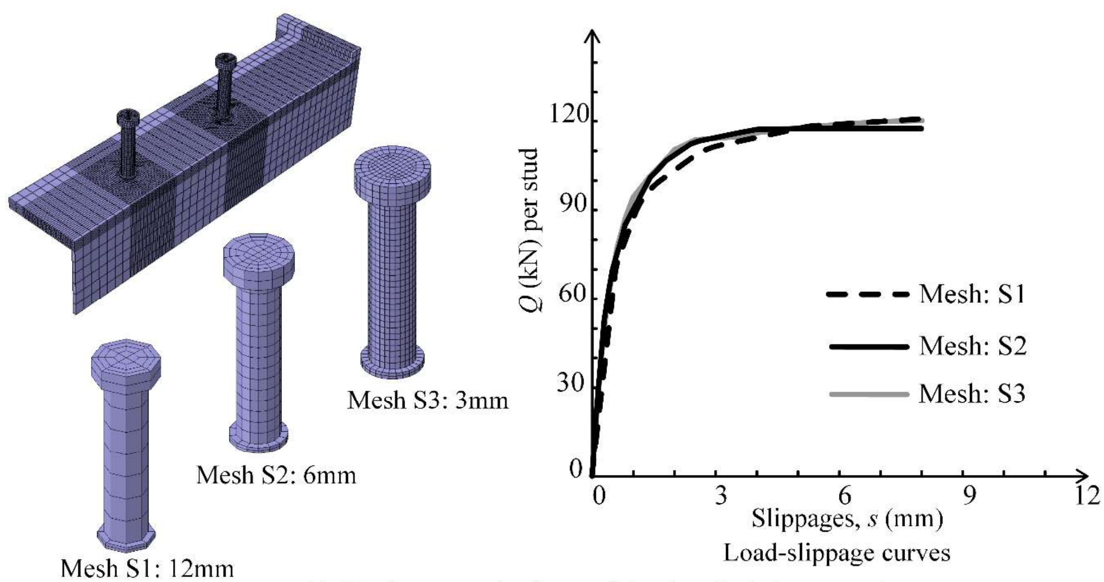

b) Various mesh sizes of the headed shear studs

Figure 6: Predicted load-slippage curves of Models SS with different element sizes

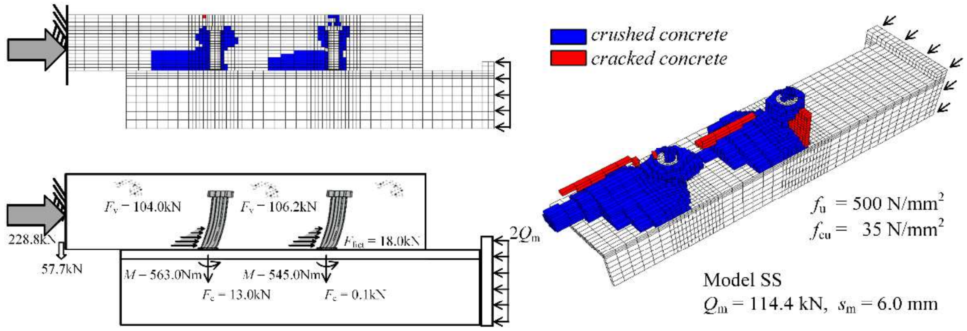

a) Model SS

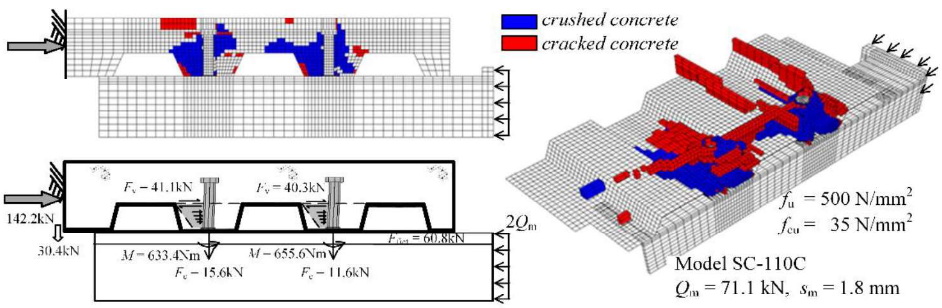

b) Model SC-110C

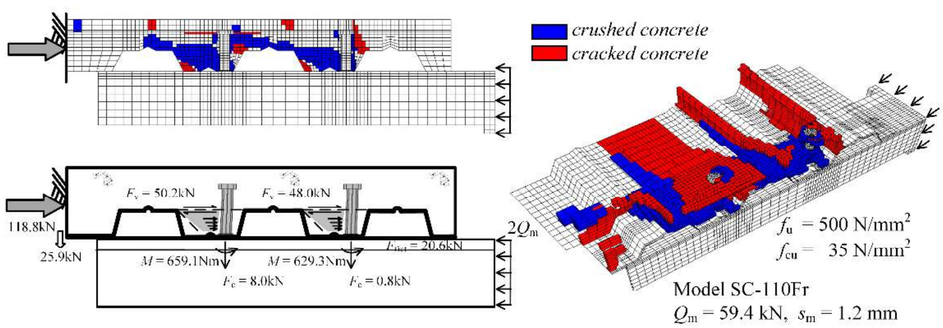

c) Model SC-110Fr

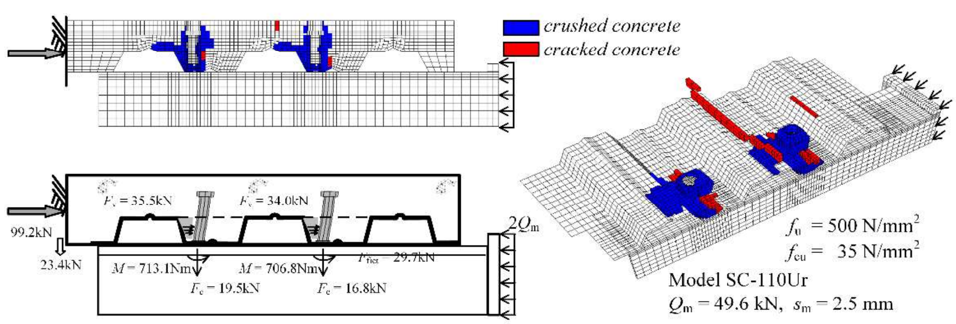

d) Model SC-110Ur

Figure 7 Distributions of damaged concrete in various models of shear connections

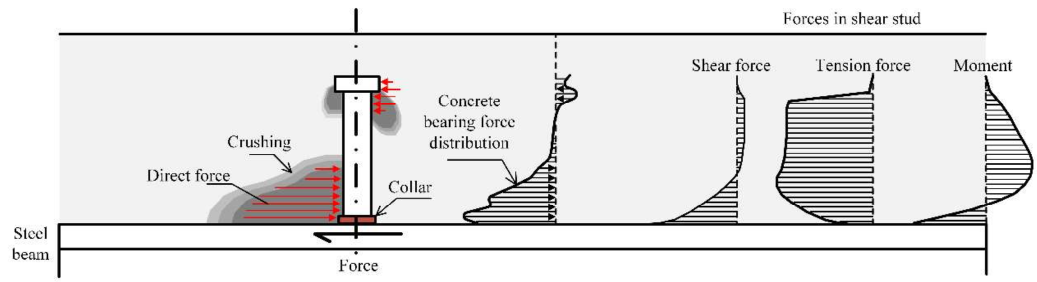

a) Shear connection with a solid concrete slab: Model SS

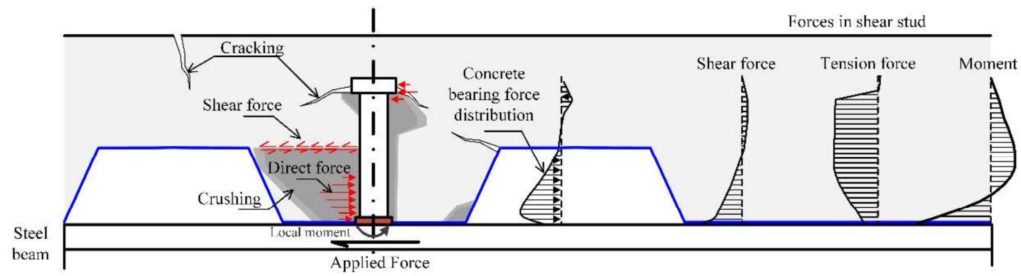

b) Shear connection with a composite slab – Central position: Model SC

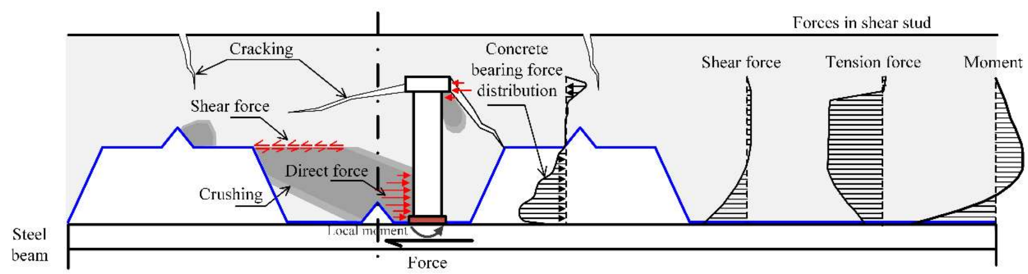

c) Shear connection with a composite slab – Favourable position: Model SCF

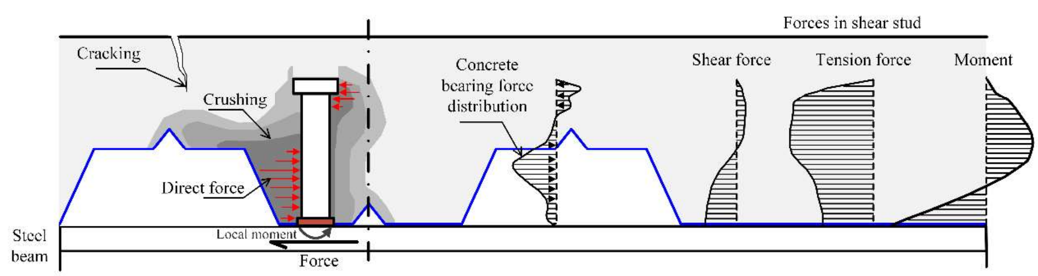

d) Shear connection with a composite slab – Unfavourable position: Model SCU

Figure 8 Load transfer mechanisms within various stud shear connections

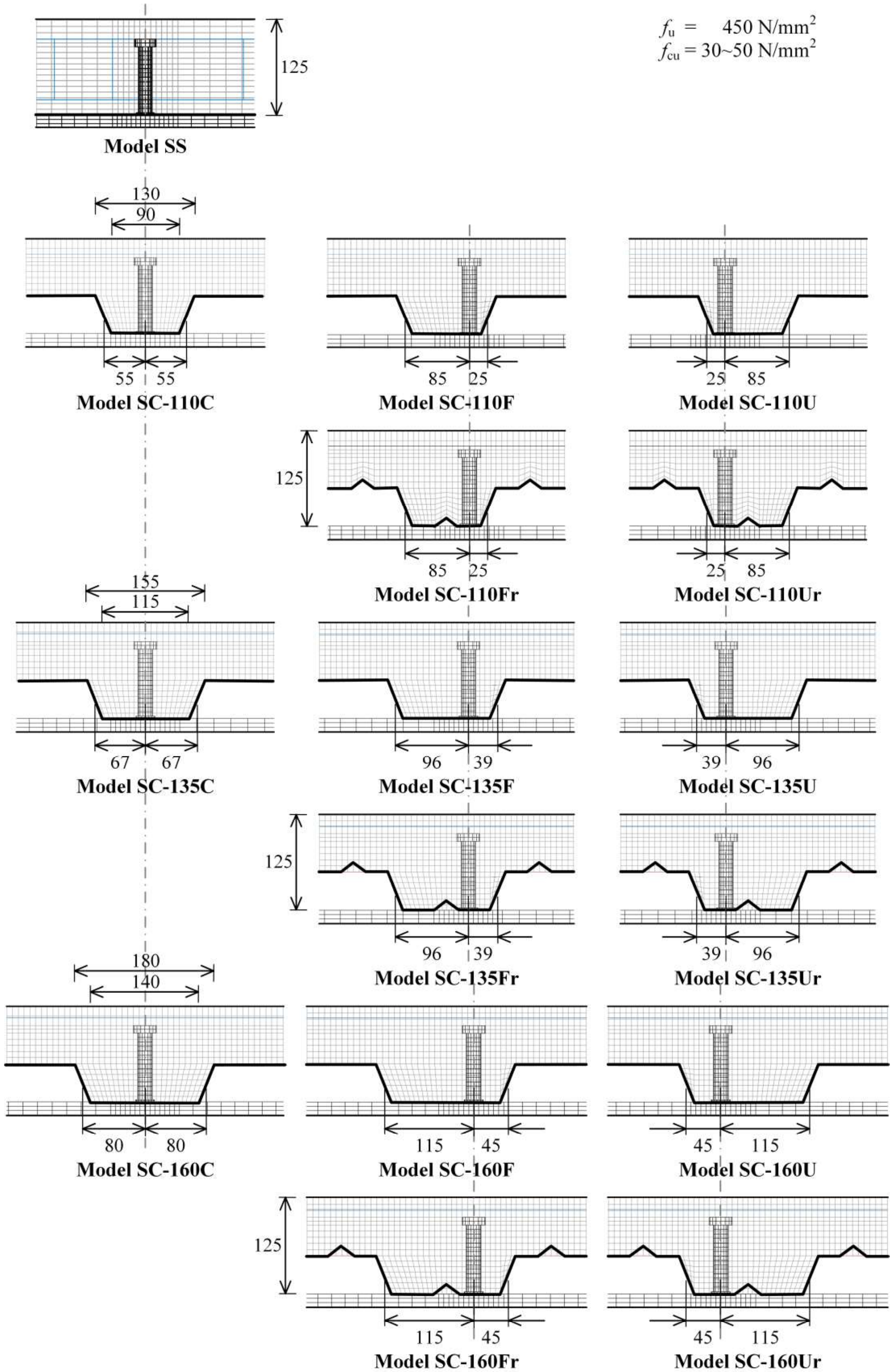

Figure 9: Finite element models of shear connections with various configurations

Parametric study: PS01

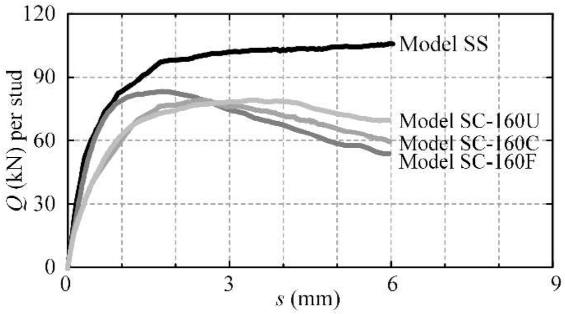

f_u = 450 N/mm^2
f_{cu} = 30 N/mm^2

b_o = 160 mm

Models	Q_m (kN)	Q_m/Q_{SS}	s_m (mm)	s_u (mm)	s_m-s_u (mm)
SS	105.1	1.00	6.0	6.0	—
SC-160F	84.5	0.80	1.8	4.0	2.2
SC-160C	76.8	0.73	2.4	5.4	3.0
SC-160U	79.1	0.75	2.1	6.0	3.9

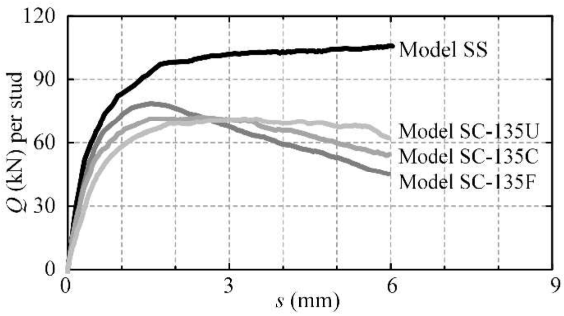

b_o = 135 mm

Models	Q_m (kN)	Q_m/Q_{SS}	s_m (mm)	s_u (mm)	s_m-s_u (mm)
SS	105.1	1.00	6.0	6.0	—
SC-135F	78.5	0.75	1.5	3.6	2.1
SC-135C	72.2	0.69	2.0	5.2	3.2
SC-135U	71.7	0.68	2.0	6.0	4.0

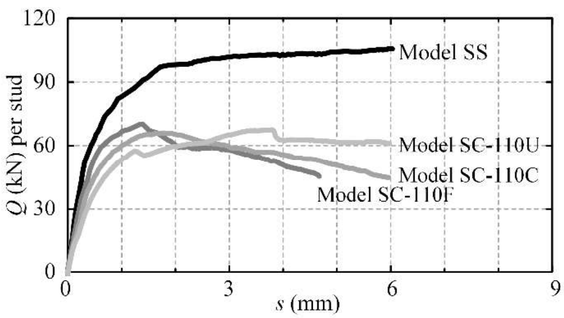

b_o = 110 mm

Models	Q_m (kN)	Q_m/Q_{SS}	s_m (mm)	s_u (mm)	s_m-s_u (mm)
SS	105.1	1.00	6.0	6.0	—
SC-110F	68.5	0.65	1.4	3.3	1.9
SC-110C	65.5	0.62	1.8	5.0	3.2
SC-110U	65.3	0.62	1.8	6.0	4.2

Figure 10: Deformation characteristics of shear connections with different installation positions and trough widths
(Positions C, F and U for b_o = 110, 135 and 160 mm)

Parametric study: PS02a with b_o = 110 mm

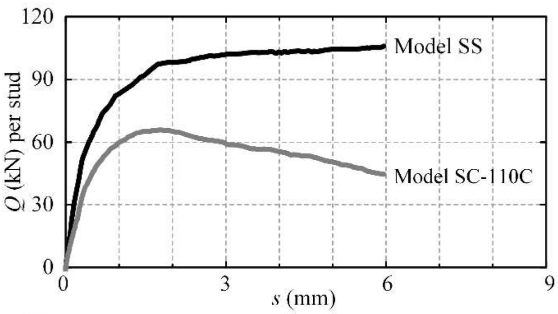

Central position

Models	Q_m (kN)	Q_m/Q_{SS}	s_m (mm)	s_u (mm)	s_u-s_m (mm)
SS	105.1	1.00	6.0	6.0	—
SC-110C	65.5	0.62	1.8	5.0	3.2

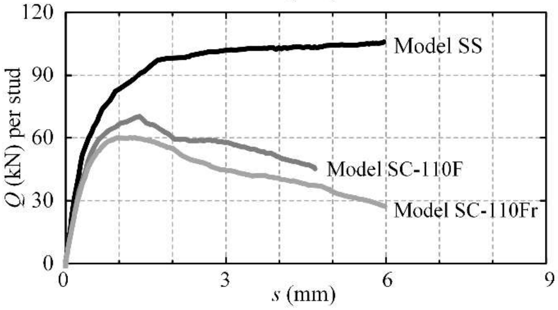

Favorable position

Models	Q_m (kN)	Q_m/Q_{SS}	s_m (mm)	s_u (mm)	s_u-s_m (mm)
SS	105.1	1.00	6.0	6.0	—
SC-110F	68.5	0.65	1.4	3.3	1.9
SC-110Fr	60.5	0.58	1.2	2.6	1.4

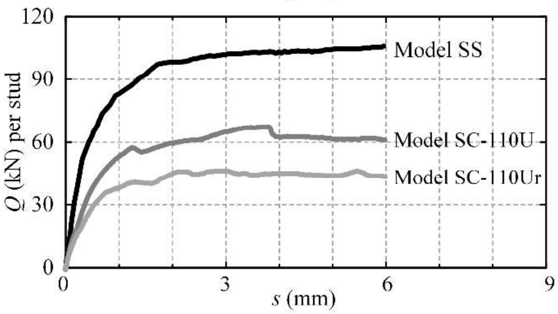

Unfavorable position

Models	Q_m (kN)	Q_m/Q_{SS}	s_m (mm)	s_u (mm)	s_u-s_m (mm)
SS	105.1	1.00	6.0	6.0	—
SC-110U	65.3	0.62	1.8	6.0	4.2
SC-110Ur	44.5	0.42	2.1	6.0	3.9

f_u = 450 N/mm^2
f_{cu} = 30 N/mm^2

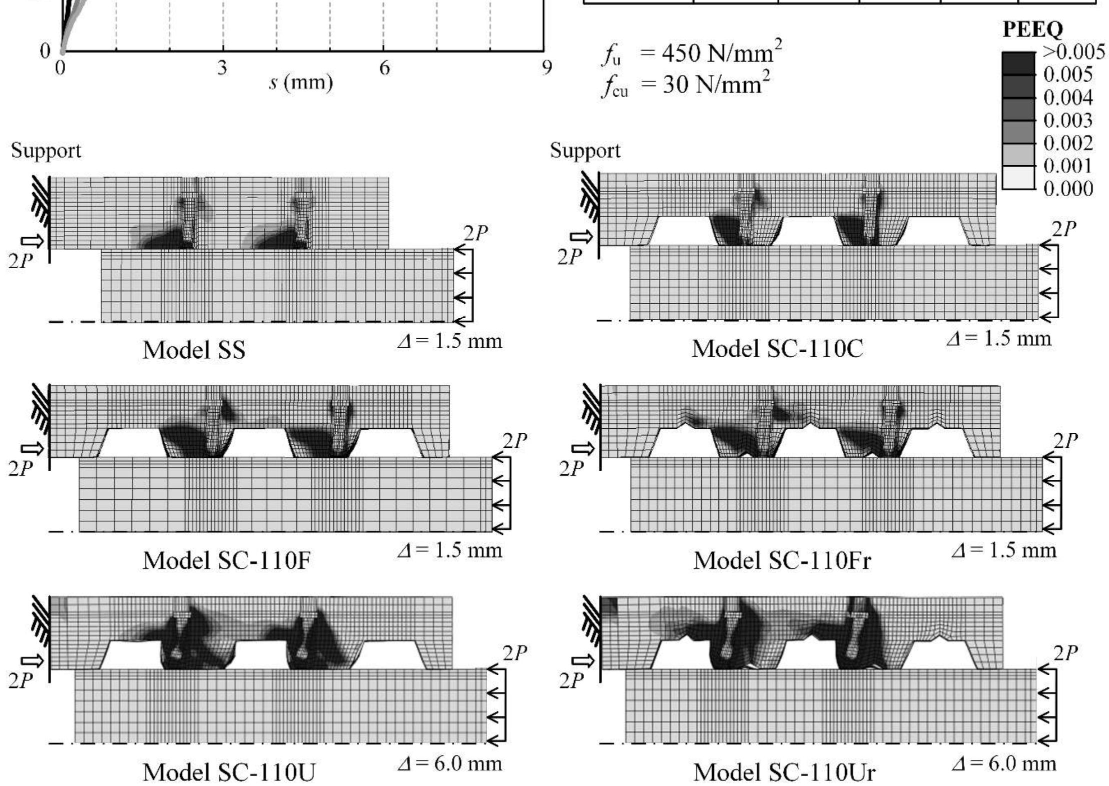

Figure 11: Numerical results of shear connections with different arrangements
(Trough width b_o at 110 mm with various cases of Positions C, F & Fr, and U & Ur)

Parametric study: PS02b with b_o = 135 mm

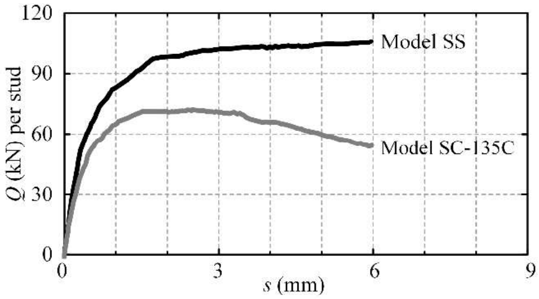

Central position

Models	Q_m (kN)	Q_m/Q_{SS}	s_m (mm)	s_u (mm)	s_u-s_m (mm)
SS	105.1	1.00	6.0	6.0	—
SC-135C	72.2	0.69	2.0	5.2	3.2

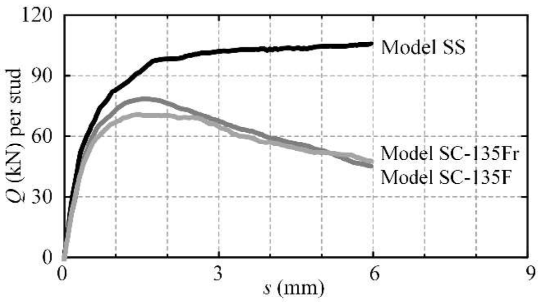

Favorable position

Models	Q_m (kN)	Q_m/Q_{SS}	s_m (mm)	s_u (mm)	s_u-s_m (mm)
SS	105.1	1.00	6.0	6.0	—
SC-135F	78.5	0.75	1.5	3.6	2.1
SC-135Fr	71.1	0.68	1.5	4.0	2.5

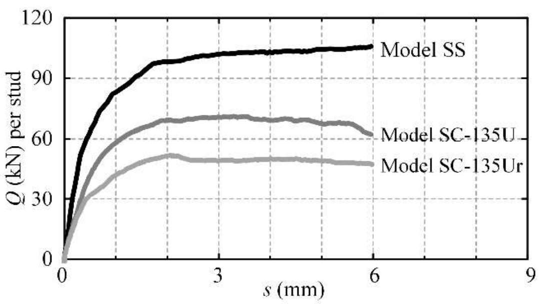

Unfavorable position

Models	Q_m (kN)	Q_m/Q_{SS}	s_m (mm)	s_u (mm)	s_u-s_m (mm)
SS	105.1	1.00	6.0	6.0	—
SC-135U	71.7	0.68	2.0	6.0	4.0
SC-135Ur	52.4	0.50	2.1	6.0	3.9

f_u = 450 N/mm^2
f_{cu} = 30 N/mm^2

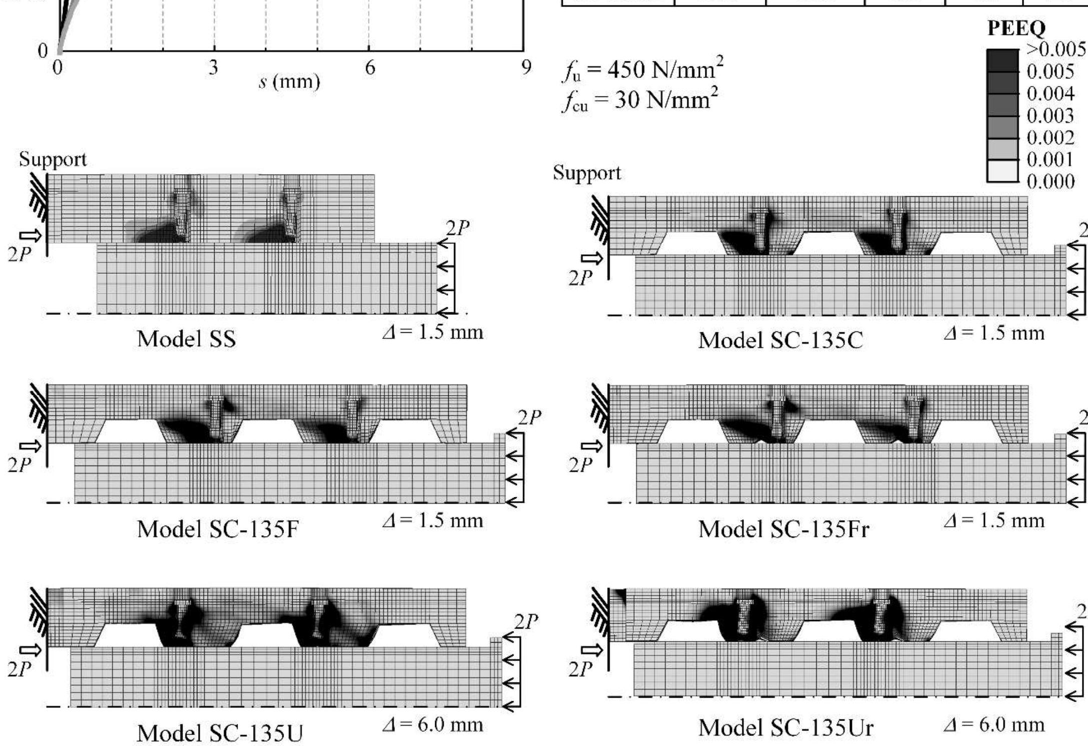

Figure 12: Numerical results of shear connections with different arrangements
(Trough width b_o at 135 mm with various cases of Positions C, F & Fr, and U & Ur)

Parametric study: PS02c with b_o = 160 mm

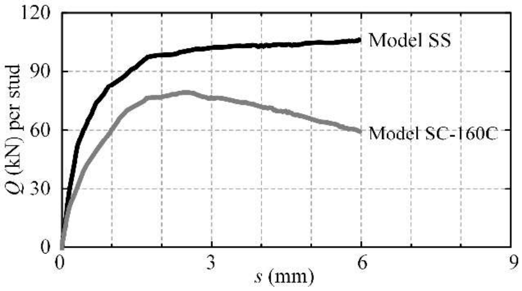

Central position

Models	Q_m (kN)	Q_m/Q_{SS}	s_m (mm)	s_u (mm)	s_u-s_m (mm)
SS	105.1	1.00	6.0	6.0	—
SC-160C	76.8	0.73	2.4	5.4	3.0

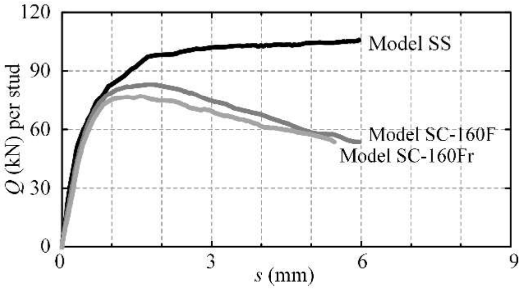

Favorable position

Models	Q_m (kN)	Q_m/Q_{SS}	s_m (mm)	s_u (mm)	s_u-s_m (mm)
SS	105.1	1.00	6.0	6.0	—
SC-160F	84.5	0.80	1.8	4.0	2.2
SC-160Fr	77.3	0.74	1.6	4.0	2.4

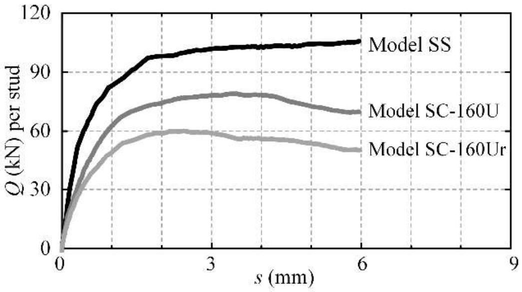

Unfavorable position

Models	Q_m (kN)	Q_m/Q_{SS}	s_m (mm)	s_u (mm)	s_u-s_m (mm)
SS	105.1	1.00	6.0	6.0	—
SC-160U	79.1	0.75	2.1	6.0	3.9
SC-160Ur	60.5	0.58	2.0	6.0	4.0

f_u = 450 N/mm^2
f_{cu} = 30 N/mm^2

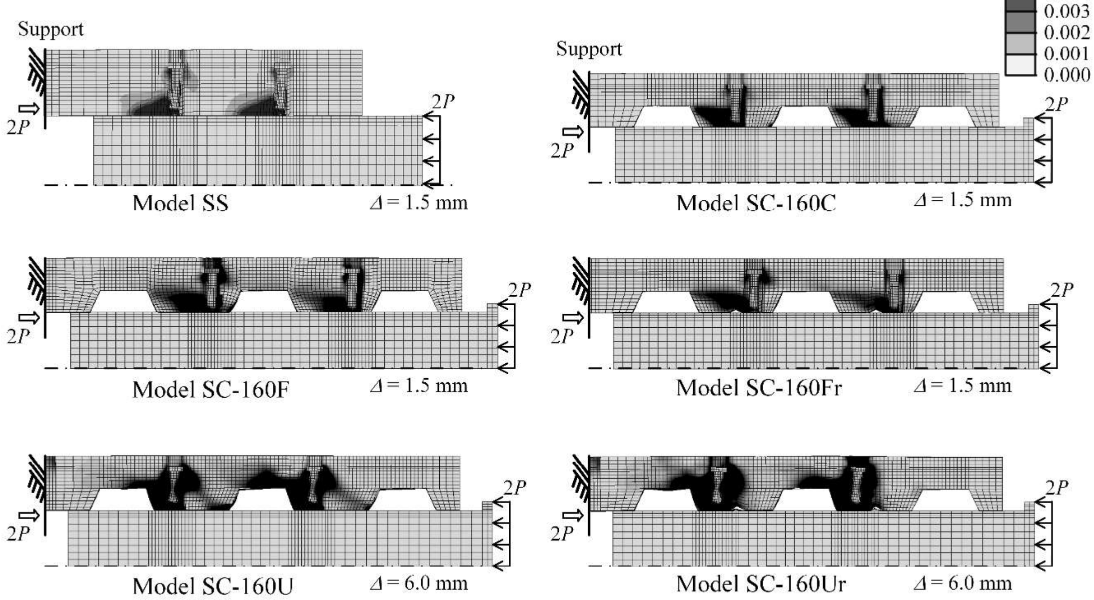

Figure 13: Numerical results of shear connections with different arrangements
(Trough width b_o at 160 mm with various cases of Positions C, F & Fr, and U & Ur)

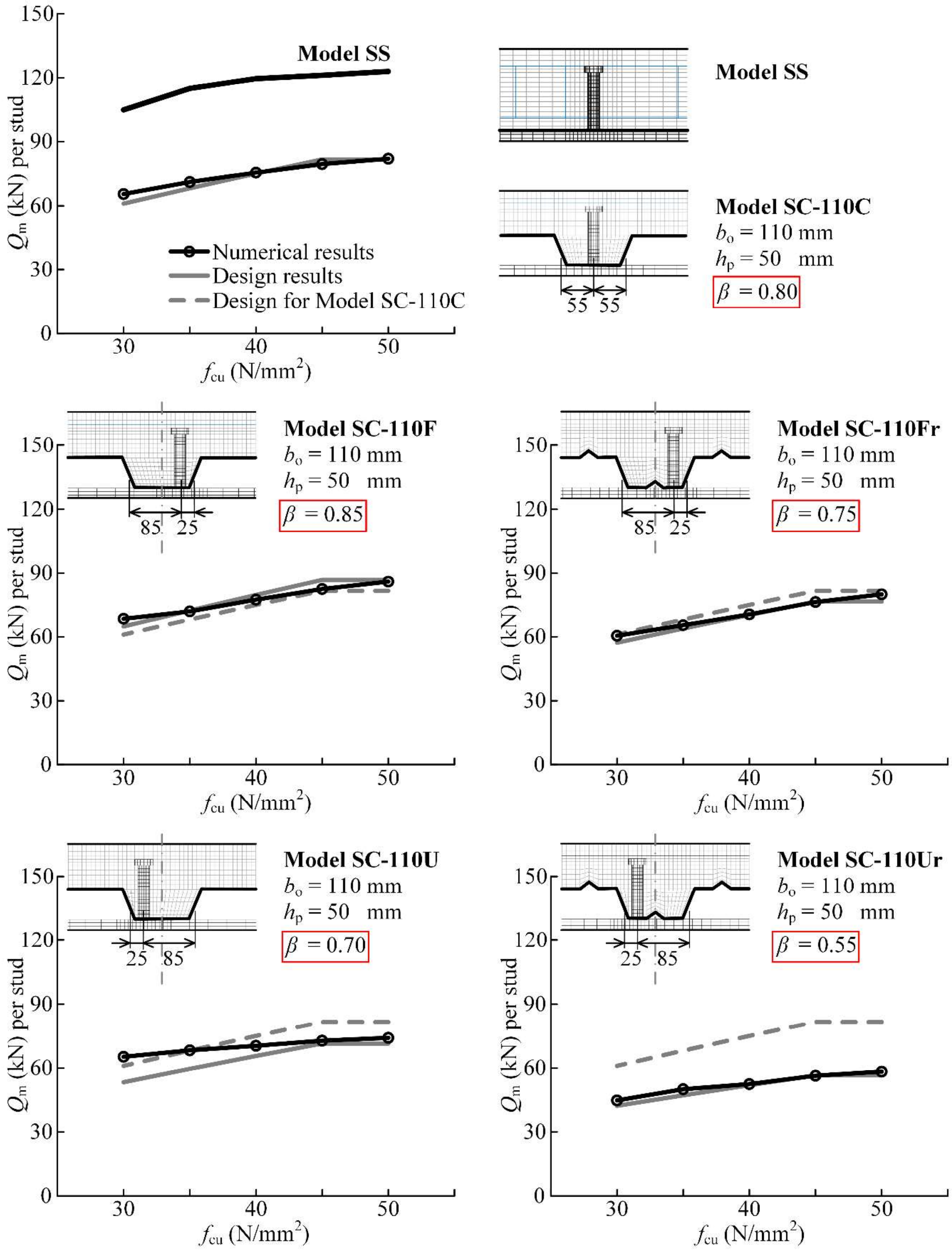

Figure 14: Shear resistances of stud shear connections with profiled decks:
Trough width b_o = 110 mm

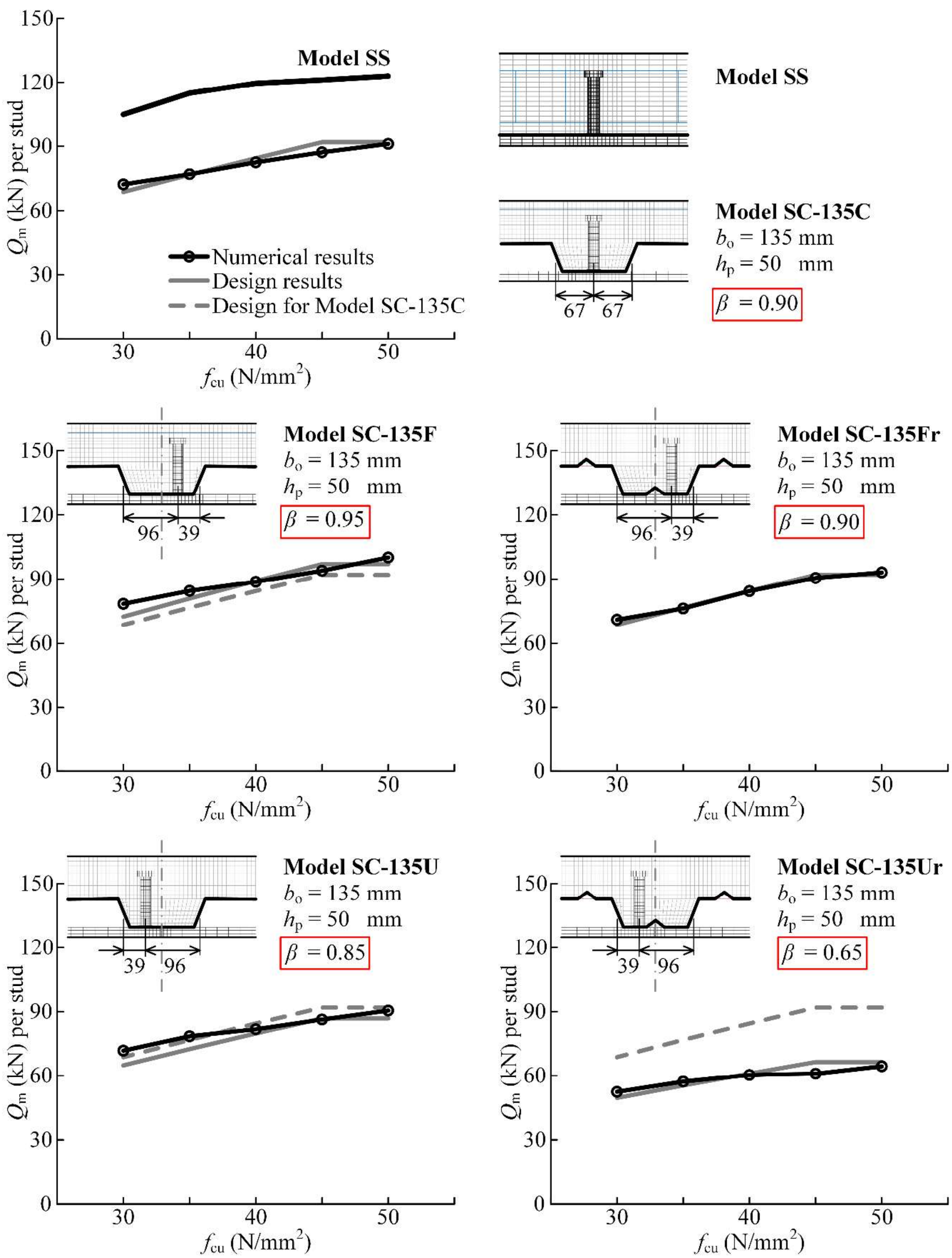

Figure 15: Shear resistances of stud shear connections with profiled decks:
Trough width b_o = 135 mm

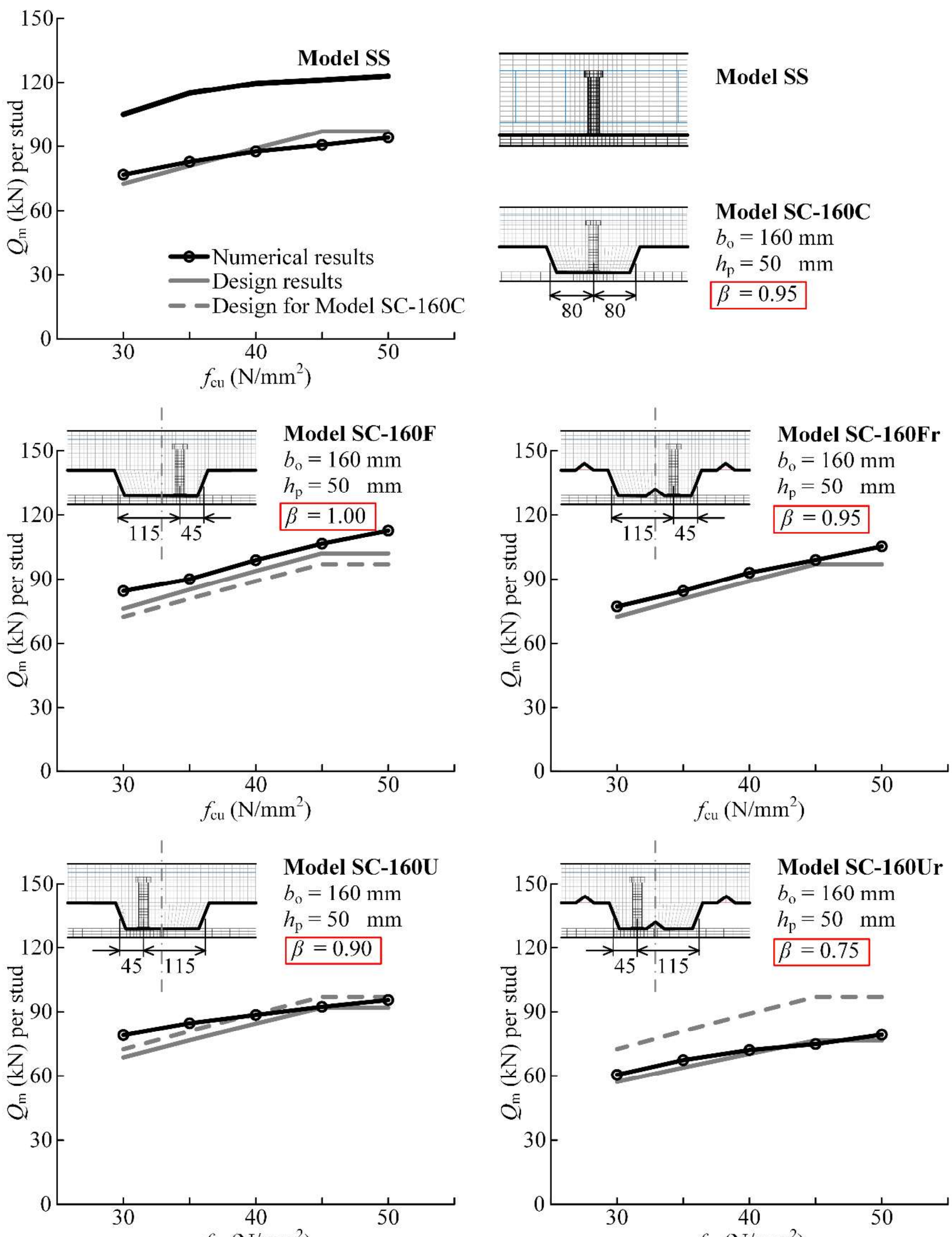

Figure 16: Shear resistance of stud shear connections with profiled decks:
Trough width b_o = 160 mm

Table 1: Measured shear resistances and ductility limits

Test Series	$\boldsymbol{Q_m}$ (kN)	s_m (mm)	Q_m/Q_{SS}
SS	121.2	6.0	1.00
SCFr	58.9	1.2	0.52
SCUr	49.6	2.5	0.43

Table 2: Summary of convergence study of Series SS with different element sizes

a) Model SS with concrete of different element sizes

Finite element meshes	Shear resistance Q_{FEM} (kN)	Relative resistance ratio	Computational time (hours)
C2-S2	120.0	1.026	0.5
C3-S2	117.6	1.005	2.7
C4-S2	117.0	1.000	21.5

b) Model SS with steel studs of different element sizes

Finite element meshes	Shear resistance Q_{FEM} (kN)	Relative resistance ratio	Computational time (hours)
C3-S1	118.4	1.010	2.0
C3-S2	117.6	1.003	2.7
C3-S3	117.2	1.000	4.6

Note: Q_{FEM} is the predicted shear resistance of the shear connection at a slippage of 6.0 mm.

Table 3: Summary of parametric studies of stud shear connections

Study PS01

Installation position of headed shear studs	Central position	Favourable position	Unfavourable position
Composite slabs	**Model SC-160C**	**Model SC-160F**	**Model SC-160U**
	Model SC-135C	**Model SC-135F**	**Model SC-135U**
	Model SC-110C	**Model SC-110F**	**Model SC-110U**
Solid concrete slabs (reference)	Model SS		

Study PS02a: b_o = 110 mm

Installation position of headed shear studs	Central position	Favourable position	Unfavourable position
Composite slabs	**Model SC-110C**	—	—
	—	**Model SC-110F**	**Model SC-110U**
	—	**Model SC-110Fr**	**Model SC-110Ur**

Study PS02b: b_o = 135 mm

Installation position of headed shear studs	Central position	Favourable position	Unfavourable position
Composite slabs	**Model SC-135C**	—	—
	—	**Model SC-135F**	**Model SC-135U**
	—	**Model SC-135Fr**	**Model SC-135Ur**

Study PS02c: b_o = 160 mm

Installation position of headed shear studs	Central position	Favourable position	Unfavourable position
Composite slabs	**Model SC-160C**	—	—
	—	**Model SC-160F**	**Model SC-160U**
	—	**Model SC-160Fr**	**Model SC-160Ur**

Table 4: Configuration parameter β

Trough width b_o (mm)	Installation positions of the shear studs				
	C	F	Fr	U	Ur
110	0.80	0.85	0.75	0.70	0.55
135	0.90	0.95	0.90	0.85	0.65
160	0.95	1.00	0.95	0.90	0.75

Notes:

"C" indicates a shear stud installed in central position of a decking trough;

"F" indicates a shear stud installed in a favourable position of a decking trough;

"U" indicates a shear stud installed in unfavourable position of a decking trough; and

"r" indicates presence of longitudinal stiffeners in the central position of a decking trough.